

Thermoacoustic-reflected focusing lens based on acoustic Bessel-like beam with phase manipulation

An-Ru Hou(侯安茹), Wen-Ting Gao(高文婷), Jiao Qian(钱姣), Hong-Xiang Sun(孙宏祥), Yong Ge(葛勇), Shou-Qi Yuan(袁寿其), Qiao-Rui Si(司乔瑞), Xiao-Jun Liu(刘晓峻)

Citation: Chin. Phys. B . 2018, 27(12): 124301. **doi:** 10.1088/1674-1056/27/12/124301
Journal homepage: http://cpb.iphy.ac.cn; http://iopscience.iop.org/cpb

What follows is a list of articles you may be interested in

Bidirectional asymmetric acoustic focusing by two flat acoustic metasurfaces

Di-Chao Chen(陈帝超), Xing-Feng Zhu(朱兴凤), Qi Wei(魏琦), Da-Jian Wu(吴大建)

Chin. Phys. B . 2018, 27(12): 124302. **doi:** 10.1088/1674-1056/27/12/124302

Broadband acoustic focusing by symmetric Airy beams with phased arrays comprised of different numbers of cavity structures

Jiao Qian(钱姣), Bo-Yang Liu(刘博阳), Hong-Xiang Sun(孙宏祥), Shou-Qi Yuan(袁寿其), Xiao-Zhu Yu(俞笑竹)

Chin. Phys. B . 2017, 26(11): 114304. **doi:** 10.1088/1674-1056/26/11/114304

Theoretical analysis of interaction between a particle and an oscillating bubble driven by ultrasound waves in liquid

Yao-Rong Wu(武耀蓉), Cheng-Hui Wang(王成会)

Chin. Phys. B . 2017, 26(11): 114303. **doi:** 10.1088/1674-1056/26/11/114303

Acoustic focusing through two layer annuluses in air

Yi-Jun Guan(管义钧), Hong-Xiang Sun(孙宏祥), Shu-Sen Liu(刘树森), Shou-Qi Yuan(袁寿其), Jian-Ping Xia(夏建平), Yong Ge(葛勇)

Chin. Phys. B . 2016, 25(10): 104302. **doi:** 10.1088/1674-1056/25/10/104302

Nonlinear impedances of thermoacoustic stacks with ordered and disordered structures

Ge Huan, Fan Li, Xia Jie, Zhang Shu-Yi, Tao Sha, Yang Yue-Tao, Zhang Hui

Chin. Phys. B . 2014, 23(7): 074301. **doi:** 10.1088/1674-1056/23/7/074301

Thermoacoustic-reflected focusing lens based on acoustic Bessel-like beam with phase manipulation*

An-Ru Hou(侯安茹)[1,†], Wen-Ting Gao(高文婷)[1,†], Jiao Qian(钱姣)[1,†], Hong-Xiang Sun(孙宏祥)[1,2,3,‡], Yong Ge(葛勇)[1,2,§], Shou-Qi Yuan(袁寿其)[1], Qiao-Rui Si(司乔瑞)[1], and Xiao-Jun Liu(刘晓峻)[2,3]

[1] *Research Center of Fluid Machinery Engineering and Technology, Faculty of Science, Jiangsu University, Zhenjiang* 212013, *China*
[2] *Key Laboratory of Modern Acoustics, Department of Physics and Collaborative Innovation Center of Advanced Microstructures, Nanjing University, Nanjing* 210093, *China*
[3] *State Key Laboratory of Acoustics, Institute of Acoustics, Chinese Academy of Sciences, Beijing* 100190, *China*

(Received 30 July 2018; revised manuscript received 30 September 2018; published online 10 November 2018)

We report the realization of broadband reflected acoustic focusing lenses based on thermoacoustic phased arrays of Bessel-like beams, in which the units of phase manipulation are composed of three rigid insulated boundaries and a thermal insulation film in air with different temperatures. Based on these units, we realize a reflected focusing lens which can focus reflected acoustic energy on a line, and its fractional bandwidth can reach about 0.29. In addition, we discuss the influences of the base angle of Bessel-like beam, the number of basic unit, and the variation of unit temperature on focusing performances in details. Furthermore, the reflected focusing lens for the cylindrical acoustic wave based on the Bessel-like beam is also demonstrated. The proposed focusing lens has the advantages of a broad working bandwidth, large focus size, and high robustness, which may provide possibilities for the design and application of acoustic lenses.

Keywords: acoustic focusing, Bessel-like beam, thermoacoustic, phase manipulation

PACS: 43.35.+d, 43.25.+y **DOI:** 10.1088/1674-1056/27/12/124301

1. Introduction

Acoustic focusing (AF) has increasingly attracted interest owing to its great potential applications in many scenarios, ranging from acoustic energy harvesting to ultrasonic medical diagnosis and treatment.[1–4] The emergences of sonic crystals (SCs),[5–7] and acoustic metamaterials[8–15] have provided more possibilities and alternative concepts to designers of AF lenses. By gradually changing the parameters of the units of SCs, the AF lenses with gradient-refractive indexes have been demonstrated.[16–19] However, the unit size is comparable to or larger than the wavelength, and thus this type of AF lens is large at low frequency. Moreover, the AF lenses fabricated by acoustic metamaterials are composed of a series of units with different negative refractive indices.[20–24] Based on small size and large negative refractive index of units, small and thin AF lenses have become possible.[25] Besides, the Mie resonances of cylinder structures,[14,26,27] the temperature gradients induced by heat sources,[28,29] the phase manipulation of metafibers[30,31] and different numbers of cavity structures,[32,33] and the interferences in metal plate with binary wave-path slits,[34] have also been introduced to realize the advanced AF lenses successively.

Recently, acoustic metasurfaces have opened a new avenue to design advanced AF lenses with subwavelength thickness and planar structure. The AF lens is realized by tailoring the phase delays in a planar structure much thinner than the working wavelength.[35–46] But most of AF lenses usually have a large acoustic impedance difference between lens materials and ambient media, which inevitably affects their working bandwidth. To overcome this problem, the units filled with air with different temperatures[47,48] and different proportions of two gases[49,50] have been proposed to fabricate the metasurfaces, which can obtain matched acoustic impedances between both media and broad working bandwidths. Most of these lenses generally focus the acoustic energy on a point,[40,46] which is not suitable for some special application scenarios. As a typical example, the sound system in a large stadium and the driving-bird equipment in an airport both need a large focusing region.[35,39] The Bessel beam proposed by Durnin[51] can realize AF on a line with non-diffracting feature. Therefore, the design of broadband AF lenses based on the Bessel-like beam is highly desired.

In this work, we propose broadband reflected AF lenses based on thermoacoustic phased arrays of Bessel-like beams. The units of phase manipulation are designed by employing air with different temperatures surrounded by three rigid insulated boundaries and a thermal insulation film. Based on these units, we design a broadband reflected AF lens which

*Project supported by the National Natural Science Foundation of China (Grant Nos. 11774137 and 51779107), the Six-Talent Peaks Project in Jiangsu Province, China (Grant No. GDZB-019), the China Postdoctoral Science Foundation (Grant No. 2017M621643), the Natural Science Foundation of Jiangsu Higher Educational Institutions of China (Grant No. 18KJB140003), and the Practice Innovation Training Program Projects for Jiangsu University (Grant No. 201710299023Z) and for the Industrial Center of Jiangsu University.

†These authors contributed equally to this work.
‡Corresponding author. E-mail: jsdxshx@ujs.edu.cn
§Corresponding author. E-mail: geyong@ujs.edu.cn

© 2018 Chinese Physical Society and IOP Publishing Ltd

can focus the reflected acoustic energy on a line, and its fractional bandwidth can reach about 0.29. We also discuss the details of the influence of the base angle of Bessel-like beam, the number of basic unit, and the variation of unit temperature on the AF performance. Moreover, the reflected AF lenses for cylindrical acoustic wave with different base angles of the Bessel-like beam are also investigated in detail.

2. Design of reflected AF lens based on acoustic Bessel-like beam

2.1. Design of Bessel beam

The reflected AF lens in this work is based on the Bessel-like beam owing to its features of line focusing and non-diffraction. Assuming an acoustic wave with the normal incidence propagates along the x direction and passes through a reflected phased array, the reflected angle θ_r (measured from the x direction) can be derived according to the generalized Snell's law[52]

$$\frac{1}{k_0}\frac{\mathrm{d}\varphi(y)}{\mathrm{d}y} = \sin\theta_r, \tag{1}$$

where $k_0 = 2\pi f/c_0$ is the wave number, c_0 is the acoustic velocity of air at 300 K, f is the frequency, and $\varphi(y)$ is the phase delay distribution of the reflected phase array along the y direction.

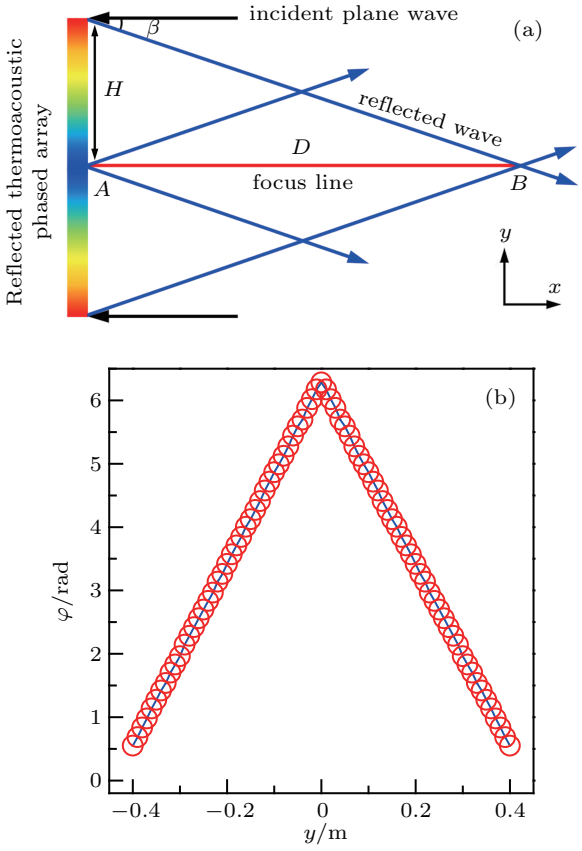


Fig. 1. (color online) (a) Schematic diagram of reflected AF lens based on Bessel-like beam. (b) Discrete phase distribution of 81 units (red hollow circles) of designed AF lens. Blue lines in panel (b) represent theoretical continuous phase delays.

To realize a reflected acoustic Bessel-like beam, the distribution of the phase delays along the y direction is expressed as[39]

$$\varphi(y) = -k_0\,|y|\sin\beta, \tag{2}$$

where β is the base angle of the Bessel-like beam. In this work, we propose a reflected AF lens consisting of a thermoacoustic phased array of the Bessel-like beam. As shown in Fig. 1(a), the incident acoustic wave (black arrows) is placed at the right side. The reflected acoustic wave is formed as the Bessel-like beam, focusing on the red line AB. The relationship between the length of the focus line (D) and the base angle β is

$$D = H/\tan\beta, \tag{3}$$

where H is the half height of the AF lens.

In the reflected thermoacoustic phased array, the parameters are selected as $y = 81$ cm, $\beta = \pi/20$, $f = 5.0$ kHz, and $c_0 = 343$ m/s. As shown in Fig. 1(b), the theoretical continuous phase delays [blue solid lines] of the Bessel-like beam can be obtained by Eq. (2), and 81 red hollow dots represent discrete phase delays of the thermoacoustic phased array.

2.2. Basic thermoacoustic theory

To realize thermoacoustic phased array, we first design a reflected thermoacoustic unit with phase manipulation. Assuming that air is the ideal fluid, the acoustic velocity c and the density ρ of air are determined by the temperature T, which are shown as follows[47]

$$c = \sqrt{\gamma RT/M}, \tag{4}$$

$$\rho = p_0 M/RT, \tag{5}$$

where $\gamma = 1.4$ is the ratio of the molar heat capacities of air, $M = 28.97 \times 10^{-3}$ kg/mol is the molar mass of air, $R = 8.31$ J/(mol/K) is the molar gas constant, and $p_0 = 101.325$ kPa is the pressure at 273 K.

2.3. Reflected thermoacoustic unit of phase manipulation

The reflected thermoacoustic unit is constructed by three rigid thermal insulation boundaries (blue solid lines) and a thermal insulation film (red dashed line) immersed in air with the temperature T, which is shown in Fig. 2(a). The thickness of the rigid thermal insulation boundary is d, and the length and width of the unit are l and h, respectively. To obtain the reflected phase delays, we design a model shown in Fig. 2(b). The acoustic wave is horizontally incident from the right side and passes through the unit with the rigid thermal insulation boundaries. At the left boundary, the acoustic wave is reflected again and returns to the outside.

Throughout this work, the acoustic characteristics are simulated by the finite element method based on COMSOL Multiphysics software, and the structure parameters of the unit are selected as $l = 8$ cm, $h = 1$ cm, $d = 0.05$ cm, and the ambient temperature $T_0 = 300$ K. Besides, we introduce the influence of temperature on the

thermal parameters of air, such as the thermal conductivity $k = -0.00227583562 + (1.15480022 \times 10^{-4}) \times T - (7.90252856 \times 10^{-8}) \times T^2 + (4.11702505 \times 10^{-11}) \times T^3 - (4.11702505 \times 10^{-15}) \times T^4$ W·m^{-1}·K^{-1} and the thermal capacity $C_p = 1047.63657 - 0.372589265 \times T + (9.45304214 \times 10^{-4}) \times T^2 - (6.02409443 \times 10^{-7}) \times T^3 + (1.2858961 \times 10^{-10}) \times T^4$ J·(kg·K)$^{-1}$. The parameters c and ρ of air can be calculated from Eqs. (4) and (5), respectively. Moreover, the heat flux of the external boundaries is continuous, and the thermal convection inside the model is neglected in the thermal simulations. Figure 2(c) shows the reflected phase delays φ of the unit with different air temperatures, in which the parameter φ is shown in the range from 0 to 2π owing to its periodicity. Note that the reflected phase delays could cover a whole 2π range in the temperature range 560 K–2450 K (shown in shaded region).

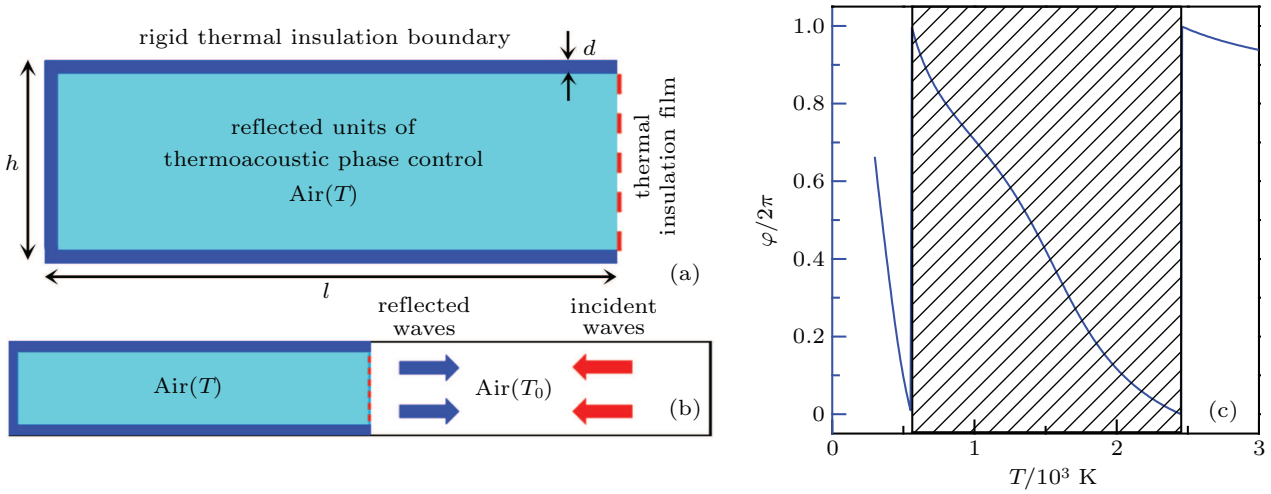


Fig. 2. (color online) (a) Reflected unit of thermoacoustic phase manipulation, and (b) numerical model for simulation of reflected phase delays. (c) Reflected phase delays of units with different temperatures.

3. Numerical results and discussions

3.1. AF performances

Figures 3(a) and 3(b) show the distributions of the reflected intensity field through the theoretical continuous phase delays and the thermoacoustic phased array, respectively. It is obvious that the reflected acoustic wave is formed as the Bessel-like beam [shown in red diamonds]. The reflected acoustic energy is focused on a line at the right side of the lens almost without diffraction. Based on Eq. (3), the theoretical length of the focus D is calculated as 2.53 m, which agrees well with the simulated result in Fig. 3(b), and is larger than that of previous AF lenses.[40–46] Furthermore, the AF characteristic induced by the thermoacoustic phased array agrees well with the theoretical result in Fig. 3(a). Moreover, it is found from Fig. 3(c) that the AF does not exist in the free space. Therefore, the reflected AF lenses with large focusing region and high performance is demonstrated based on the Bessel-like beam.

To clearly exhibit the AF performances, the transverse and longitudinal distributions of the acoustic intensities [lines I–IV in Figs. 3(b) and 3(c)] are simulated, which is shown in Fig. 4. Note that, with the thermoacoustic lens, the centre position of the focus is (124.1 cm, 0), the maximum intensity at the center of the focus is about 6 times than that in the free space. Besides, as shown in Fig. 4(a), the intensity along the line I (from 0.5 m to 2.5 m) is larger than 3.0 Pa^2, showing a high performance of line focusing. Furthermore, it is found from Fig. 4(b) that the acoustic energy is mainly focused at

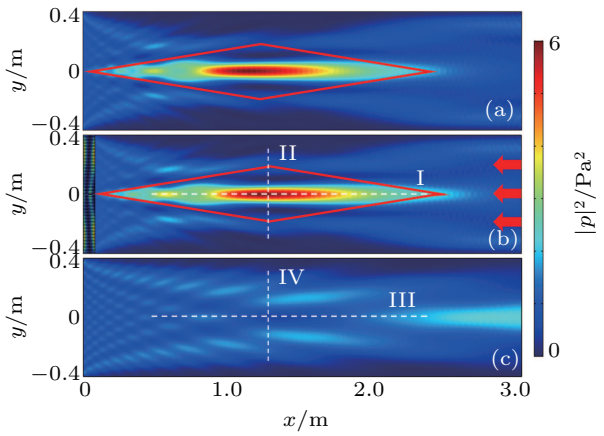


Fig. 3. (color online) Spatial distributions of reflected intensity field for Bessel-like beam induced by (a) theoretical continuous phase delays and (b) thermoacoustic phased array, and (c) for free space at 5.0 kHz. Red arrows in panel (b) refer to incident acoustic waves.

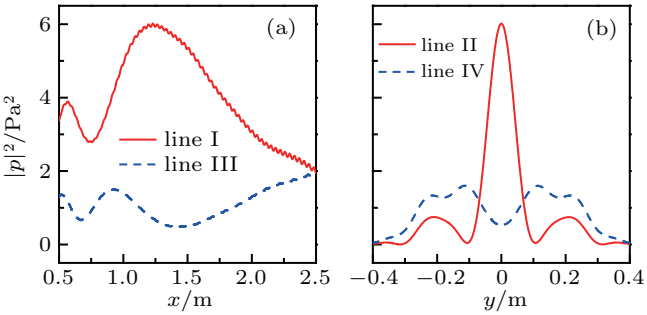


Fig. 4. (color online) Distributions of reflected intensity through (a) lines I and III, and (b) lines II and IV in Fig. 3.

the position $y = 0$, and the diffraction is very weak, showing obvious non-diffracting characteristic of the AF lens.

3.2. Broad working bandwidth

To show the bandwidth of the AF lens, we simulate the distributions of the reflected intensity field at different frequencies, which is shown in Fig. 5. It is found that, at three selected frequencies, the reflected acoustic energy is also focused on a line at the right side. Thus, the working bandwidth of the lens reaches more than 1.4 kHz, and the fractional bandwidth (the ratio of the bandwidth to the center frequency) is about 0.29. Besides, with the increase of the frequency, the focus position moves to the right. This characteristic is also shown in Fig. 6. Such a phenomenon results from the fact that the incident angle and the phase distribution of the lens are the same. By increasing the frequency, the reflected angle θ_r decreases based on Eq. (1), and therefore the focus length increases. Based on these results, we deduce that the proposed AF lens has the advantages of s broad bandwidth and an adjustable focus position.

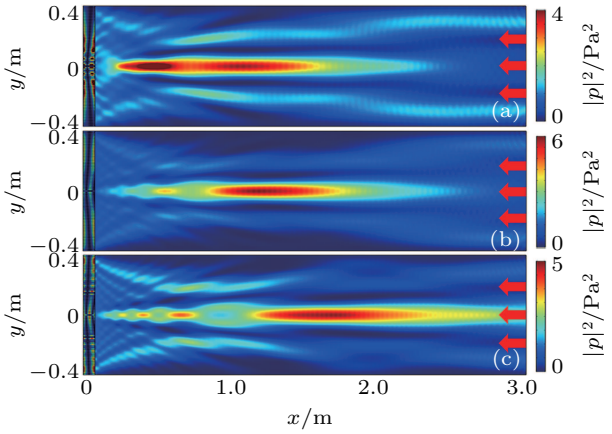


Fig. 5. (color online) Spatial distributions of reflected intensity field induced by reflected AF lens at (a) 4.2 kHz, (b) 4.9 kHz, and (c) 5.6 kHz. Red arrows refer to incident acoustic waves.

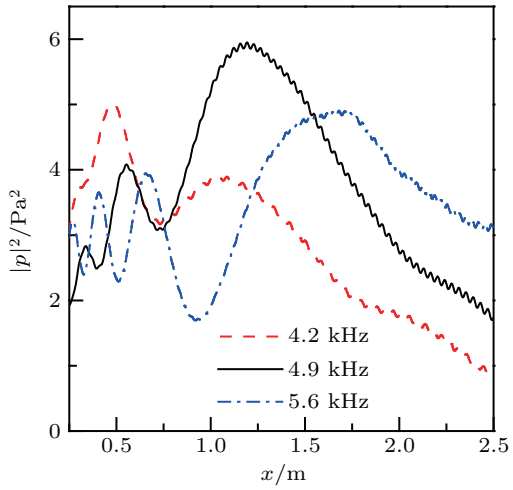


Fig. 6. (color online) Transverse distributions of reflected intensity through focus induced by reflected AF lens at different frequencies.

3.3. Influence of base angle of Bessel-like beam on AF performances

We also study the influence of the base angle β of the Bessel-like beam on the AF performance. Figures 7(a)–7(c) show the theoretical continuous phase delays (blue line) and discrete phase delays (red hollow dots) of the reflected AF lenses with different β. The distributions of the acoustic intensity field induced by the reflected AF lenses with $\beta = 6°$, 12°, and 15° are shown in Figs. 7(d)–7(f), respectively. It is obvious that the Bessel-like beam and the AF effect still exist with different β. The focal length and the focus size decrease gradually with the increase of β, which can be explained by Eq. (3). Therefore, the focus energy is more concentrated and the focus position moves to the left gradually. The transverse distributions of the reflected intensity through the focus with different β are shown in Fig. 8.

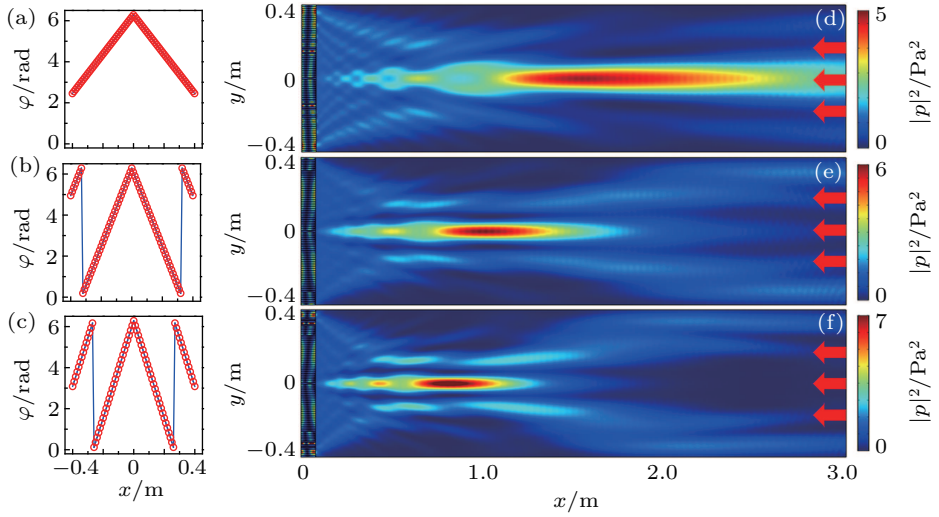


Fig. 7. (color online) Theoretical continuous phase delays (blue line) and discrete phase delays (red hollow dots) of reflected AF lenses with base angles (a) 6°, (b) 12°, and (c) 15°. Spatial distributions of reflected intensity field induced by reflected AF lenses with base angles (d) 6°, (e) 12°, and (f) 15° at 5.0 kHz. Red arrows in panels (d), (e), and (f) refer to incident acoustic waves.

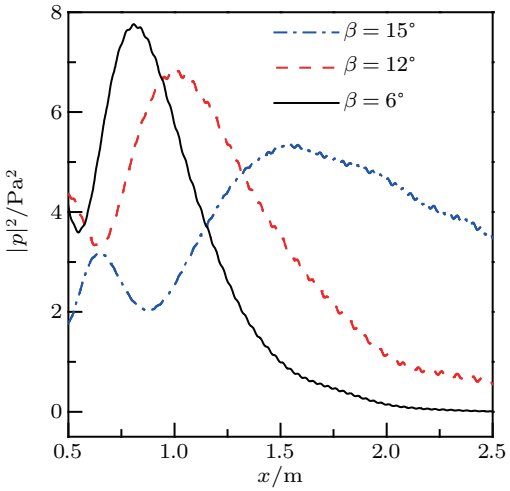


Fig. 8. (color online) Transverse distributions of reflected intensity through the focus with different values of β.

We also find that, with the increase of β, the intensity at the focus increases, and the focus position moves to the left, which arises from the fact that the refraction angles of two transmitted beams increases, and the interference region moves to the left and becomes small. Therefore, the acoustic energy is more concentrated, which agrees with that in Fig. 7.

3.4. Robustness of an AF lens

To demonstrate the robustness of a reflected AF lens, we separately adopt four, six, and eight types of basic reflected units with different air temperatures to design the AF lenses with 81 discrete phase delays (red hollow dots), in which the phase delay distributions are displayed in Figs. 9(a)–9(c). As shown in Figs. 9(d)–9(f), the Bessel-like beam and the AF effect still exist for three cases, and the reflected acoustic energy is also focused on a line at the right side. Note that with more basic reflected units, the maximum intensity at the focus increases slightly, and the characteristics of the focus almost remain unchanged.

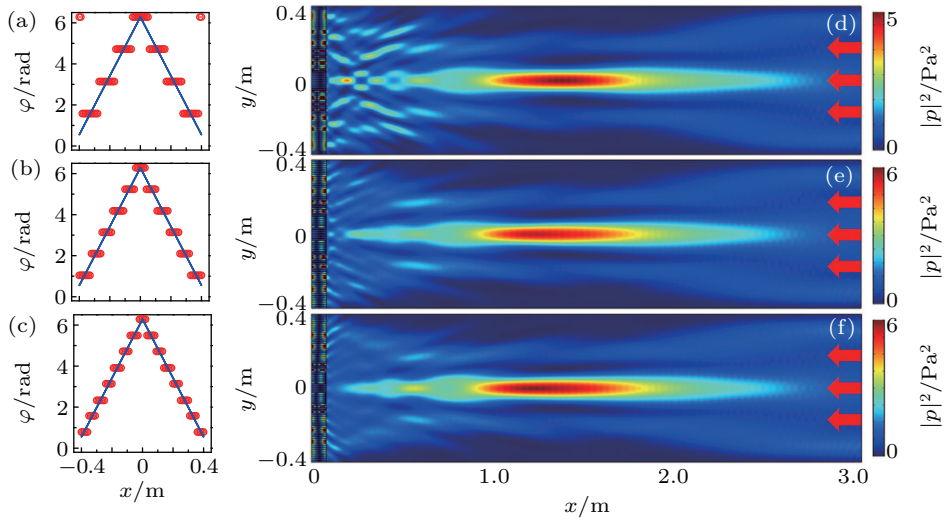


Fig. 9. (color online) Theoretical continuous phase delays (blue line) and discrete phase delays (red hollow dots) of reflected AF lenses based on (a) four, (b) six, and (c) eight types of reflected units. Spatial distributions of reflected intensity field induced by reflected AF lenses with (d) four, (e) six, and (f) eight types of reflected units at 5.0 kHz. Red arrows in panels (d), (e), and (f) refer to incident acoustic waves.

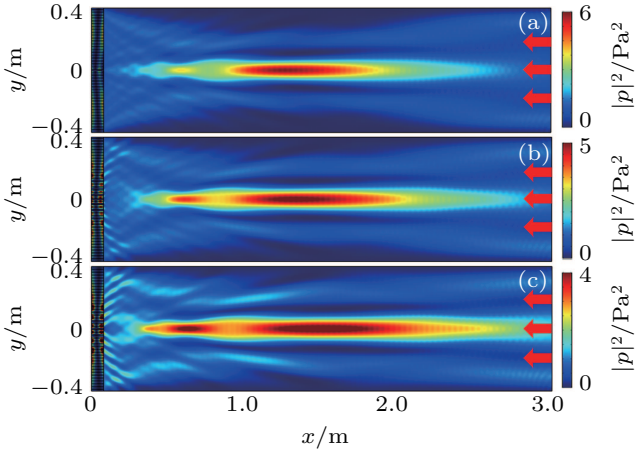


Fig. 10. (color online) Spatial distributions of reflected intensity field induced by reflected AF lenses in Fig. 3(b) by increasing temperatures of units (a) $100T$, (b) $300T$, and (c) $500T$ at 5.0 kHz. Red arrows in panels (a), (b), and (c) refer to incident acoustic waves.

Figures 10(a)–10(c) show the distributions of the intensity field induced by the thermoacoustic phased array, in which the temperatures of all units increase $100T$, $300T$, and $500T$, respectively, and the other parameters are the same as those in Fig. 3(b). It is obvious that, with the increase of the temperatures of all units, the lens also has high AF performance, and the focus position remains the same, but the intensity of the focus decreases slightly. The aforementioned results verify the high robustness of the proposed reflected AF lens.

3.5. Reflected AF lens for cylindrical acoustic wave

Based on the generalized Snell's law, we also realize a reflected AF lens based on the Bessel-like beam for a cylindrical acoustic wave. As shown in Fig. 11, the position of the incident cylindrical wave is located at (25 cm, 0), and the re-

flected acoustic wave induced by the cylindrical acoustic wave is formed as Bessel-like beam, and is focused on a line at the right side. The phase delay $\varphi(y)$ of the thermoacoustic phased array for the cylindrical acoustic wave satisfies

$$\varphi(y) = -k_0(|y|\sin\beta + \sqrt{y^2+L^2}), \tag{6}$$

where L is the distance between the positions of the cylindrical acoustic source and the lens.

The theoretical continuous phase delays (blue lines) and the 81 discrete phase delays (red hollow dots) of the AF lenses for the cylindrical acoustic wave with different base angles are shown in Figs. 12(a)–12(c), in which the parameter L is selected as 0.25 m. Figures 12(d)–12(f) show the spatial distributions of the reflected intensity field induced by the designed AF lenses with $\beta = 6°$, 12°, and 15°, respectively. It is obvious that the reflected acoustic energy induced by the proposed AF lenses for the cylindrical acoustic wave is also formed as the Bessel-like beam and is focused on a line at the right side. With the increase of β, the focus size decreases, and the focus position moves to the left gradually; which are similar with those in Fig. 7.

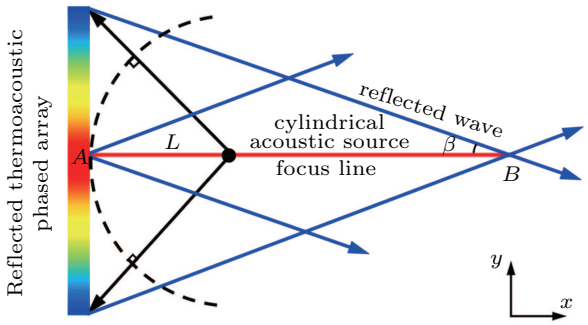


Fig. 11. (color online) Schematic diagram of reflected AF lens for cylindrical acoustic wave.

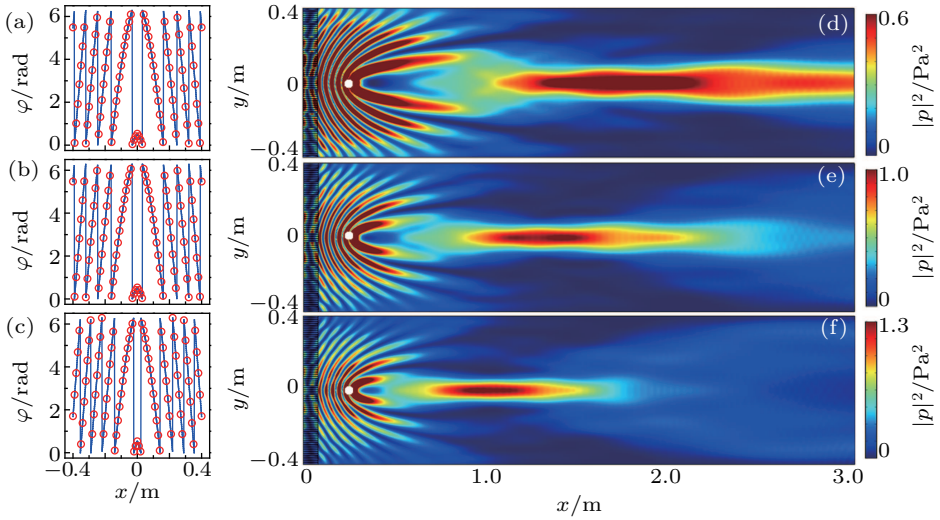


Fig. 12. (color online) Theoretical continuous phase delays (blue line) and discrete phase delays (red hollow dots) of reflected AF lenses for cylindrical acoustic wave with base angles (a) 6°, (b) 12°, and (c) 15°. Spatial distributions of reflected intensity field induced by reflected AF lenses for cylindrical acoustic wave with base angles (d) 6°, (e) 12°, and (f) 15° at 5.0 kHz. White dots in panels (d), (e), and (f) refer to cylindrical acoustic source.

4. Conclusion

In conclusion, we have demonstrated broadband reflected AF lenses for both plane and cylindrical acoustic waves based on Bessel-like beams. In the reflected thermoacoustic phased arrays, each unit consists of three rigid insulated boundaries and a thermal insulation film in air with different temperatures, and its reflected phase delays could cover the whole 2π range. Based on the units, a broadband reflected AF lens is realized. The results show that the fractional bandwidth can reach about 0.29 and the length of the focus reaches about 2.53 m, which is larger than that of previous AF lenses. The focus size and the focal length both decrease gradually with the increase of the base angle, and the maximum intensity at the focus increases slightly with more basic units, but the focus characteristics almost remain unchanged. Furthermore, the reflected AF lenses for the cylindrical acoustic wave are also realized. The proposed AF lens has the advantages of broad working bandwidth, large focus size, and high robustness, which provides more mechanisms for acoustic manipulation and extends its potential applications in acoustic lenses.

References

[1] Li J S, Fok L, Yin X B, Bartal G and Zhang X 2009 *Nat. Mater.* **8** 931
[2] Yan X, Zhu R, Huang G L and Yuan F G 2013 *Appl. Phys. Lett.* **103** 121901
[3] Gu Y, Cheng Y and Liu X J 2015 *Appl. Phys. Lett.* **107** 133503
[4] Zheng L and Guo J Z 2016 *Acta Phys. Sin.* **65** 044305 (in Chinese)
[5] Liu Z Y, Zhang X X, Mao Y W, Zhu Y Y, Yang Z Y, Chan C T and Sheng P 2000 *Science* **289** 1734
[6] Torrent D and Sanchez-Dehesa J 2010 *Phys. Rev. Lett.* **105** 174301
[7] Lu J Y, Qiu C Y, Ke M Z and Liu Z Y 2016 *Phys. Rev. Lett.* **116** 093901
[8] Lai Y, Wu Y, Sheng P and Zhang Z Q 2011 *Nat. Mater.* **10** 620
[9] Liang Z and Li J 2012 *Phys. Rev. Lett.* **108** 114301
[10] Fleury R, Sounas D L, Sieck C F, Haberman M R and Alù A 2014 *Science* **343** 516

[11] Xie Y B, Wang W Q, Chen H Y, Konneker A, Popa B I and Cummer S A 2014 *Nat. Commun.* **5** 5553

[12] Duan Y T, Luo J, Wang G H, Hang Z H, Hou B, Li J, Sheng P and Lai Y 2015 *Sci. Rep.* **5** 12139

[13] Cheng Y, Zhou C, Yuan B G, Wu D J, Wei Q and Liu X J 2015 *Nat. Mater.* **14** 1013

[14] Zhang Z W, Wei Q, Cheng Y, Zhang T, Wu D J and Liu X J 2017 *Phys. Rev. Lett.* **118** 084303

[15] Liu C K, Luo J and Lai Y 2018 *Phys. Rev. Mater.* **2** UNSP 045201

[16] Deng K, Ding Y Q, He Z J, Zhao H P, Shi J and Liu Z Y 2009 *J. Phys. D: Appl. Phys.* **42** 185505

[17] Lin S C S, Huang T J, Sun J H and Wu T T 2009 *Phys. Rev. B* **79** 094302

[18] Martin T P, Nicholas M, Orris G J, Cai L W, Torrent D and Sánchez-Dehesa J 2010 *Appl. Phys. Lett.* **97** 113503

[19] Peng S S, He Z J, Jia H, Zhang A Q, Qiu C Y, Ke M Z and Liu Z Y 2010 *Appl. Phys. Lett.* **96** 263502

[20] Zhang S, Yin L L and Fang N 2009 *Phys. Rev. Lett.* **102** 194301

[21] Zigoneanu L, Popa B I and Cummer S A 2011 *Phys. Rev. B* **84** 024305

[22] Li Y, Liang B, Tao X, Zhu X F, Zou X Y and Cheng J C 2012 *Appl. Phys. Lett.* **101** 233508

[23] Li Y, Yu G K, L B, Z X, Li G Y, Cheng S and Cheng J C 2015 *Sci. Rep.* **4** 6830

[24] Lu G X, Ding E L, Wang Y Y, Ping X Y, Cui J, Liu X Z and Liu X J 2017 *Appl. Phys. Lett.* **110** 123507

[25] Molerón M and Daraio C 2015 *Nat. Commun.* **6** 8037

[26] Xia J P and Sun H X 2015 *Appl. Phys. Lett.* **106** 063505

[27] Xia J P, Sun H X, Cheng Q, Xu Z, Chen H, Yuan S Q, Zhang S Y, Ge Y and Guan Y J 2016 *Appl. Phys. Express* **9** 057301

[28] Ge Y, Sun H X, Liu C, Qian J, Yuan S Q, Xia J P, Guan Y J and Zhang S Y 2016 *Appl. Phys. Express* **9** 066701

[29] Liu C, Sun H X, Yuan S Q and Xia J P 2016 *Acta Phys. Sin.* **65** 044303 (in Chinese)

[30] Qian J, Xia J P, Sun H X, Yuan S Q, Ge Y and Yu X Z 2017 *J. Appl. Phys.* **122** 244501

[31] Qian J, Liu B Y, Sun H X, Yuan S Q and Yu X Z 2017 *Chin. Phys. B* **26** 114304

[32] Xia J P, Sun H X, Yuan S Q 2017 *Sci. Rep.* **7** 8151

[33] Sun H X, Chen J H, Ge Y, Yuan S Q and Liu X J 2018 *J. Phys. D: Appl. Phys.* **51** 245102

[34] Sun H X, Huang Y L, Xia J P and Yuan S Q 2017 *J. Phys. D: Appl. Phys.* **50** 35LT02

[35] Li Y, Liang B, Gu Z M, Zou X Y and Cheng J C 2013 *Sci. Rep.* **3** 2546

[36] Wang W Q, Xie Y B, Konneker A, Popa B I and Cummer S A 2014 *Appl. Phys. Lett.* **105** 101904

[37] Tang K, Qiu C Y, Ke M Z, Lu J Y, Ye Y T and Liu Z Y 2015 *Sci. Rep.* **4** 6517

[38] Li Y, Jiang X, Liang B, Cheng J C and Zhang L K 2015 *Phys. Rev. Appl.* **4** 024003

[39] Tian Y, Wei Q, Cheng Y, Xu Z and Liu X J 2015 *Appl. Phys. Lett.* **107** 221906

[40] Yuan B G, Cheng Y and Liu X J 2015 *Appl. Phys. Express* **8** 027301

[41] Jahdali R A and Wu Y 2016 *Appl. Phys. Lett.* **108** 031902

[42] Fan X D, Zhu Y F, Liang B, Yang J and Cheng J C 2016 *Appl. Phys. Lett.* **109** 243501

[43] Gao H, Gu Z M, Liang B, Zou X Y, Yang J, Yang J and Cheng J C 2016 *Appl. Phys. Lett.* **108** 073501

[44] Tian Y, Wei Q, Cheng Y and Liu X J 2017 *Appl. Phys. Lett.* **110** 191901

[45] Lan J, Li Y F and Liu X Z 2017 *Sci. Rep.* **7** 10587

[46] Xia J P, Zhang X T, Sun H X, Yuan S Q, Qian J and Ge Y 2018 *Phys. Rev. Appl.* **10** 014016

[47] Liu C, Xia J P, Sun H X and Yuan S Q 2017 *J. Phys. D: Appl. Phys.* **50** 505101

[48] Liu C, Sun H X, Yuan S Q, Xia J P and Qian J 2017 *Acta Phys. Sin.* **66** 154302 (in Chinese)

[49] Mei J and Wu Y 2014 *New J. Phys.* **16** 123007

[50] Wang X P, Wan L L, Chen T N, Song A L and Wang F 2016 *J. Appl. Phys.* **120** 014902

[51] Durnin J, Miceli J J and Eberly J H 1987 *Phys. Rev. Lett.* **58** 1499

[52] Yu N F, Genevet P, Kats M A, Aieta F, Tetienne J P, Capasso F and Gaburro Z 2011 *Science* **334** 333